AIChE

Equations to Predict Precipitation Onset and Bubblepoint Pressures of Asphaltenic Reservoir Fluids

J. M. del Rio, E. Ramirez-Jaramillo, and C. Lira-Galeana
R&D Branch on Flow Assurance, Mexican Institute of Petroleum, Eje Central Lazaro Cardenas 152, Col. San Bartolo Atepehuacan, Mexico City 07730, Mexico

DOI 10.1002/aic.11902
Published online June 8, 2009 in Wiley InterScience (www.interscience.wiley.com).

A set of algebraic equations to predict upper onset-of-precipitation and bubble-point pressures of asphaltene-containing reservoir fluids in wide temperature ranges are proposed. In developing the equations, laboratory data of 11 Mexican and 12 more live oils have been analyzed, and a correlation of these data with temperature has been found. A modified least-squares regression method has been used to develop two versions of the proposed equations. In one version, a single pressure/temperature data point is required to predict the entire onset/bubble-point curves at any temperature. For oils with no experimental precipitation data available at all, a second version of the proposed expressions employs standard chromatographic data of the reservoir fluid to provide a reasonable prediction. The average absolute deviations in calculated onset and bubble-point pressures by the proposed equations are 2.53 and 0.45MPa by the one-point correlations, respectively, and 3.96 and 1.62 MPa by the compositionally-based correlations, respectively. The developed expressions are simple and can be used to provide reasonable predictions of upper onset and bubble-point pressures of asphaltenic live oils in cases where laboratory data are scarce. © 2009 American Institute of Chemical Engineers *AIChE J,* 55: 1814–1822, 2009

Keywords: asphaltene precipitation envelopes, correlating equations, flow assurance

Introduction

Asphaltenes are a complex class of compounds that comprise the heaviest and more polar fraction of petroleum. The phase behavior of asphaltenic fluids resembles that of a colloidal dispersion. Upon changes in pressure, temperature or petroleum composition, asphaltenes aggregate from the oil mixture, leading to precipitation/deposition phenomena in the form of a heavy liquid/solid phase. Asphaltene precipitation, either in the reservoir, oil wells or transportation tubing, produces undesirable depositions that affect flow assurance. The phase diagram of asphaltene precipitation in oil is called asphaltene precipitation envelope[1] (APE, see Figure 1). The APE of a reservoir fluid is a valuable piece of information for flow assurance studies. Production engineers, therefore, should avoid any flow path in their wells lying within the oil's APE, otherwise, precipitation/depositions may occur, affecting well-productivity and production economics in a significant manner.

Published APE data of reservoir fluids are extremely scarce. These data may be obtained in the laboratory using sophisticated PVT equipment.[2,3] The time required to measure a complete APE for a reservoir fluid may range between 3–6 weeks, depending on sample restoration. Moreover, the laboratory protocol for reliable APE measurements involves the recovery of pressure-preserved live oil samples, whose collection in the field, for a number of reasons, may

Correspondence concerning this article should be addressed to C. Lira-Galeana at clira@inp.mx

© 2009 American Institute of Chemical Engineers

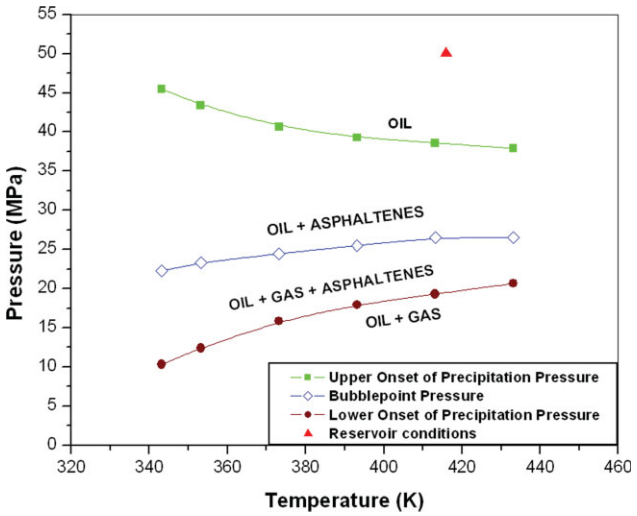

Figure 1. Measured asphaltene precipitation envelope of a Mexican reservoir fluid (Shields, 2000).

[Color figure can be viewed in the online issue, which is available at www.interscience.wiley.com.]

not always be warranted. Thus, a fast and easy method for estimating APE data of reservoir fluids is highly desirable.

In a recent work, Fahim[4,5] proposed two equations for calculating upper onset and bubble-point pressures of a number of live oils. To develop his equations, Fahim used experimental APE data[6] of various live oils from different parts of the world, but mostly from the Middle East, with different amounts of asphaltenes. His working expressions, which contain 15–17 model parameters, are functions of system temperature, crude oil composition, molecular weight, and the API gravity of the heptanes-plus fraction. When compared to the experimental onset/bubble points from which his correlations were developed, Fahim showed a good agreement with the experimental data.

Here, we used Fahim's general ideas in developing a set of simple equations to predict onset/bubble-point pressures of reservoir fluids of a broader diversity, using a minimum of experimental information. Our analysis begins with a study of the topology of the upper onset/bubble-point-pressure behavior of several crude oils with temperature. A general correlation of these variables (onset/bubble-point-pressures), which proved validity with data of 11 Mexican and 12 live oils studied by Fahim, was found. From this correlation, two different versions of the proposed equations are proposed. It is shown that either version of the proposed expressions provides accurate values of upper onset and bubble-point precipitation pressures of asphaltenic live oils.

Experimental Data Set

Table 1 shows experimental upper onset-of-precipitation and bubblepoint pressure data of 11 live oils produced in different regions of Mexico, with GOR and °API values ranging from 30–215 m^3/m^3 and 14–36, respectively. These data were measured over the past years in our laboratory,[7] using a set of extended PVT experiments. Details on the laboratory protocols followed in these experiments have been reported elsewhere.[8,9] Here, only a brief outline of these tests is presented. In a typical experiment, both the upper onset and bubble-point pressure data are measured in a constant composition expansion experiment (CCE),[10] using a temperature-controlled PVT visual cell equipped with a solids detection system. The detection system consists of a Neon-based laser-light source, and two fiber-optic probes (source and detector). The cell measures the sudden decay of light transmittance (onset of asphaltene precipitation) when the CCE experiment is carried out. Starting from, say, the reservoir conditions, the first (sharp) transmittance decay measures the upper onset of precipitation pressure. Further expansion to lower pressures displays a second light decrease at the bubblepoint. Repeated measurements at lower-temperatures allow for the tracing of the full upper onset and bubble-point pressure boundaries of an APE. In Flow Assurance studies, these pressures, when compared to the reservoir inflow and multiphase flow path in the well, can help determine whether precipitations may occur, either in the reservoir or the production tubing of the well.[11]

Figure 2a shows the measured upper onset of asphaltene precipitation pressures for 9 out of the 11 Mexican live oils shown in Table 1 (wells 3–11). From these data, a correlation analysis was performed. From various functional forms, we then found that if the T/P^{upp} ratio of each oil is plotted with respect to system temperature (as in Figure 2b), a set of nearly straight lines of the general form

$$\frac{T}{P^{upp}} = f^{upp}(C_{upp}) + B^{upp}\,T \tag{1}$$

are obtained. In Eq. 1, B^{upp} is the common slope for all straights, while $f^{upp}(\boldsymbol{C}_{upp})$ is a particular intercept, which we will make function of oil composition, C_{upp} later. In practice, B^{upp} and individual values of $f^{upp}(C_{upp})$ for each crude are computed by a modified least-squares regression procedure outlined in the Appendix (Eqs. A15–A16). Then, if the experimental values of $T/P^{upp} - f^{upp}(C_{upp})$ vs. T for each oil are plotted for all nine Mexican and 12 more live oils studied by Fahim,[3,4] Figure 2c shows that the data of *all* 21 reservoir fluid systems display a well-trended, straight-line functional behavior. As a result, one can solve Eq. 1 for $P^{upp}(T)$ to give

$$P^{upp}(T) = \frac{T}{f^{upp}(C_{upp}) + B^{upp}\,T} \tag{2}$$

Since B^{upp} is a constant, one may correlate $f^{upp}(\boldsymbol{C}_{upp})$ with oil composition through the following composition vector

$$C_{upp} = \left(x_{H_2S},\ x_{N_2},\ x_{CO_2},\ x_{C_{1-4}},\ t_{sat},\ t_{arom},\ t_{res},\ t_{asph}\right) \tag{3}$$

where x_{H_2S}, x_{N_2}, x_{CO_2} and $x_{C_1\text{-}C4}$ are the oil's mole fractions of light gases H_2S, N_2 and CO2, respectively. $x_{C_{1-4}}$ are the mole fractions of the (lumped) C_1(methane) to C_4 (iso and normal butane) light ends, and t_{sat}, t_{arom}, t_{res} and t_{asph} are the weight fractions of the lumped saturated, aromatic, resin and asphaltene fractions of the stock-tank oil, as reported in a typical SARA analysis, respectively.[12]

A first-order Taylor expansion for $f^{upp}(\boldsymbol{C}_{upp})$ around $\boldsymbol{C}_{upp} = \boldsymbol{0}$ yields

$$f^{upp}(C_{upp}) = f^{upp}(\boldsymbol{0}) + \nabla f^{upp}(\boldsymbol{0})\,C_{upp} \tag{4}$$

Table 1. Experimental Upper Onset and Bubble-Point Pressure Data of 11 Mexican Live Oils

Asphaltene precipitation data of Mexican live oils								
Well 1			Well 2			Well 3		
Temperature K		P^{bp} Mpa	Temperature K		P^{bp} Mpa	Temperature K	P^{upp} Mpa	P^{bp} Mpa
308,15		4,83	333,15		15,51	348,15	38,61	14,48
333,15		5,45	358,15		17,37	363,15	37,92	16,55
358,15		6,76	383,15		18,55	393,15	35,85	17,93
383,15		8,45				413,15	35,58	19,31
Well 4			Well 5			Well 6		
Temperature K	P^{upp} Mpa	P^{bp} Mpa	Temperature K	P^{upp} Mpa	P^{bp} Mpa	Temperature K	P^{upp} Mpa	P^{bp} Mpa
333,15		21,51	353,15	42,06	27,23	313,15	38,75	10,34
343,15	45,51	22,27	373,15	37,92	27,92	353,15	36,54	13,79
353,15	43,44	23,34	393,15		28,41	373,15	35,85	15,17
373,15	40,68	24,48	418,15		31,72	403,15	33,78	17,24
393,15	39,30	25,51				433,15	31,72	17,93
413,15	38,61	26,54						
433,15	37,92	26,54						
Well 7			Well 8			Well 9		
Temperature K	P^{upp} Mpa	P^{bp} Mpa	Temperature K	P^{upp} Mpa	P^{bp} Mpa	Temperature K	P^{upp} Mpa	P^{bp} Mpa
303,15	91,07	10,49	303,15	79,34	10,82	303,15		10,53
345,15		12,83	345,15	59,61	13,24	345,15	81,63	12,74
387,15	44,26	15,13	387,15	59,18	15,50	387,15	66,80	15,14
428,15	35,01	16,85	428,15	58,75	17,33	428,15	61,20	16,96
Well 10			Well 11					
Temperature K	P^{upp}	P^{bp} Mpa	Temperature K	P^{pp} Mpa				
333,15	37,23	16,69	313,15	54,72				
353,15	35,71	17,93	348,15	47,59				
373,15	33,09	19,31	393,15	44,62				
393,15	32,41	20,68	426,15	41,36				
413,15	31,72	21,37						

Since a null-component of $\boldsymbol{C}_{upp}$ in Eq. 3 does not contribute to the value of $f^{upp}(\boldsymbol{C}_{upp})$, one can write

$$f^{upp}(\mathbf{0}) = \mathbf{0} \tag{5}$$

Hence, by assuming that $\nabla f^{upp}(\mathbf{0})$ is a component vector of the form

$$\nabla f^{upp}(\mathbf{0}) = (f^{upp}_{H_2S}, f^{upp}_{N_2}, f^{upp}_{CO_2}, f^{upp}_{C_{1-4}}, f^{upp}_{sat}, f^{upp}_{arom}, f^{upp}_{res}, f^{upp}_{asph}) \tag{6}$$

$f^{upp}(\boldsymbol{C}_{upp})$, can, thus, be written as

$$f^{upp}(C_{upp}) = f^{upp}_{H_2S} x_{H_2S} + f^{upp}_{N_2} x_{N_2} + f^{upp}_{CO_2} x_{CO_2} + f^{upp}_{C_{1-4}} x_{C_{1-4}} + \\ + f^{upp}_{sat} t_{sat} + f^{upp}_{arom} t_{arom} + f^{upp}_{res} t_{res} + f^{upp}_{asph} t_{asph} \tag{7}$$

Equation 7 describes the composition dependence of $f^{upp}(C_{upp})$ for a reservoir fluid. Note that, for Eq. 7, compositional data commonly obtained through standard high-temperature gas-liquid (HTGLC), and high-performance liquid (HPLC-SARA) chromatography tests of the reservoir and stock-tank oils is required. We will return to this equation later.

In our analysis of the bubble-point data shown in Table 1, a similar treatment than that followed by Eq. 2 was carried out. First, we noted that the plot in Figure 3a has a similar trend than that of the parallel straights of Figure 2a, i.e., a common slope B^{bp} may exist for the whole set (see Figure 3b). Thus, all curves in Figure 3a may be represented by the general expression

$$P^{bp} = f^{bp}(C_{bp}) + B^{bp} T \tag{8}$$

In Eq. 8, $f^{bp}(\boldsymbol{C}_{bp})$ is a particular intercept, which depends on the oil in consideration. Similar to Eqs. 1–7, we have calculated a common value for B^{bp} from Eq. A15 of the Appendix, and from this slope and the experimental bubble points, individual values of the $f^{bp}(\boldsymbol{C}_{bp})$ intercept for each crude by using Eq. A16 have been calculated. Finally, we have

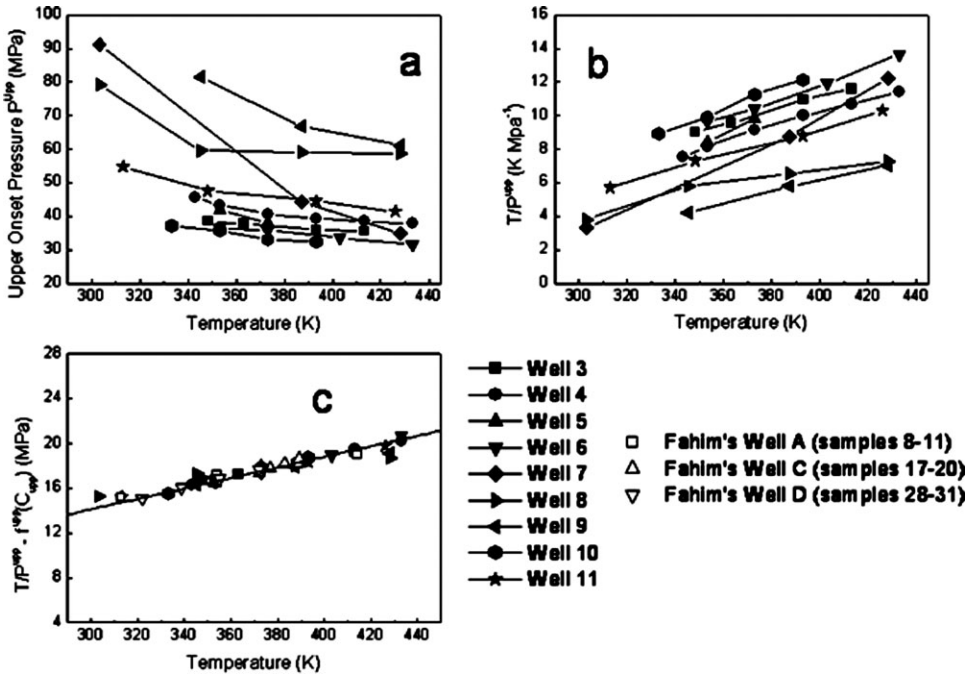

Figure 2. Asphaltene precipitation data of live oils: (a) Upper onset-of-precipitation pressures, P^{upp}, of nine Mexican live oils as a function of temperature, (b) the T/P^{upp} vs. T relationships of live-oil fluids in (a), as a function of temperature; and (c) the T/P^{upp} - $f^{upp}(C_{upp})$ straight-line correlation for the nine Mexican and 12 other (from Fahim[4]), reservoir fluids, as a function of temperature.

The straight line in 2c has a universal slope, B^{upp} equal to 0.047.

written $f^{bp}(\boldsymbol{C}_{bp})$ in Eq. 8 by the following composition-dependent expression

$$f^{bp}(C_{bp}) = f^{bp}_{H_2S}x_{H_2S} + f^{bp}_{N_2}x_{N_2} + f^{bp}_{CO_2}x_{CO_2} + \\ + f^{bp}_{sat}t_{sat} + f^{bp}_{arom}t_{arom} + f^{bp}_{res}t_{res} + f^{bp}_{asp}t_{asp} \qquad (9)$$

Equation 9 describes the composition dependence of $f^{bp}(C_{bp})$ for an asphaltene-containing live oil fluid. In Eq. 9, the (lumped) C_1-C_4 gas-content of a reservoir fluid proved to contribute little to the statistical properties of this equation and, for simplicity, was excluded from its functional form.

Results and Discussion

Table 2 shows live and stock-tank SARA compositions as reported in HTGLC and HPLC analyses of each one of the reservoir fluids shown in Table 1. These compositions were used to correlate the $f^{upp}(\boldsymbol{C}_{upp})$ and $f^{bp}(C_{bp})$ parameters in Eqs. 7 and 9, respectively. Table 3a shows the final values of the equation coefficients, together with global values for the slopes B^{upp} and B^{bp}. In the regression process, we noted that the coefficient values change slightly (particularly those for $f^{upp}(\boldsymbol{C}_{upp})$), when data of a particular oil was arbitrarily withdrawn from the data set. Table 3b presents the change in calculated coefficients for Eqs. 2 and 7 for P^{upp}, and 8-9 for P^{bp}, as a result of the withdrawal procedure (Well 3). The effect of data withdrawal (prediction capability) or inclusion (correlation) in calculated results will be shown later.

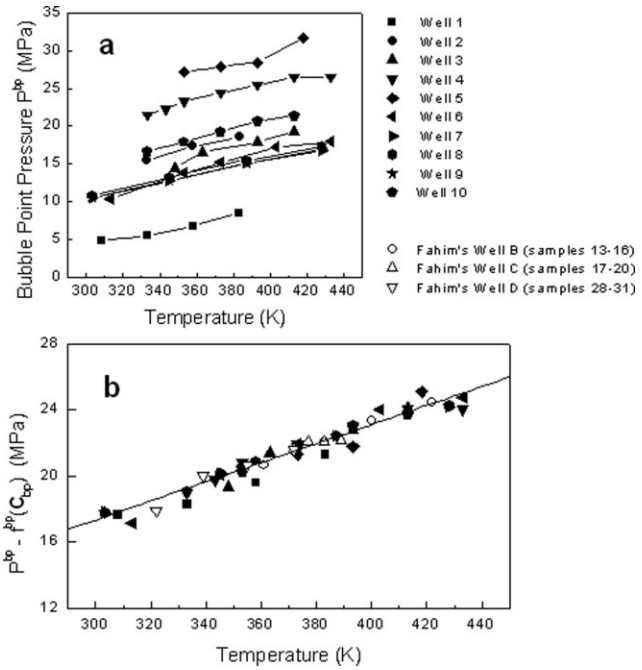

Figure 3. (a) Bubble-point pressures P^{bp}, of the 10 Mexican reservoir fluids of Table 1, as a function of temperature, (b) the P^{sat} - f^{sat}(Csat) straight-line correlation for the 10 Mexican and 12 other (from Fahim[4]) reservoir fluids, as a function of temperature.

The straight line in Figure 3b has a universal slope, B^{bp} equal to 0.0578.

Table 2. Reservoir Fluid Light-Ends and Stock-Tank SARA Compositions, and $f^{upp}(C_{upp})$ and $f^{bp}(C_{bp})$ Values for Each One of the Oils shown in Table 1

	Mixture composition									
Well	x_{H_2S} Mole %	x_{N_2} Mole %	x_{CO_2} Mole %	$x_{C_1\text{-}C_4}$ Mole %	t_{sat} Wt%	t_{arom} Wt%	t_{res} Wt%	t_{asph} Wt%	f^{upp} (C_{upp}) K Mpa^{-1}	f^{bp} (C_{bp}) K Mpa^{-1}
well 1	0	0,4	1,4	47,34	31,5	49,49	14,3	4,06		−12,8296
well 2	0	0,75	1,72	46,75	36,12	45,78	14,06	3,04		−3,5487
well 3	5,39	0,91	1,57	50,35	54,67	28,89	13,36	3,08	−7,6938	−4,8569
well 4	0,35	0,28	6,7	44,87	33,63	37,21	14,33	14,83	−8,7878	2,5059
well 5	5,25	1,15	1,48	49,76	59,28	30,58	9,41	0,73	−8,0980	6,6097
well 6	0,08	0,66	1,03	45,99	43,87	43,29	9,74	3,1	−7,0365	−6,7832
well 7	0,02	0,71	1,05	59,77	46,89	33,07	17,3	2,72	−9,5731	−7,3176
well 8	0,12	0,7	1,2	56,51	44,65	34,55	14,9	2,86	−11,4865	−6,9189
well 9	0,02	0,63	1,05	59,2	46,48	34,34	17,74	1,43	−12,6651	−7,2982
well 10	1,44	0,47	1,59	61,83	55,14	30,73	11,42	4,21	−6,6555	1,3653
well 11	1,14	0,83	0	66,04	60,53	32,63	6,32	0,52	−9,5098	

Figure 4 compares the experimentally-determined (black circles) values of for Wells 3–11, together with calculated onset pressures by the proposed Eqs. 2 and 7 (full line), with correlation parameters from Table 3a, showing a good agreement. The average absolute deviation (AAD) defined as

$$AAD = \frac{1}{n}\sum_{i=1}^{n}\left|(P_i^{upp})_{calc} - (P_i^{upp})_{\exp}\right| \quad (10)$$

was calculated, where n is the total number of experimental onset points, and $(P_i^{upp})_{calc}$ and $(P_i^{upp})_{\exp}$ are the calculated, and experimental precipitation pressures at different temperatures, respectively. The lefthand column in Table 4 shows the calculated AAD's for each Well. An average AAD of 3.96 MPa (correlation option) was obtained. As can be seen from both Figure 4 and Table 4, Wells 7 and 8 resulted with the less-accurate estimations, most probably due to experimental uncertainties. If results from Wells 7 and 8 were removed from the computed average, the resulting AAD improves to a value of 1.65 MPa.

To test the predictive capability of Eqs. 2 and 7, data of Well 3 were excluded from the regression, and data of only Wells 4–11 were used to obtain the equation parameters. Table 3b shows the calculated parameters from this reduction in the data set. Predicted results compared to the experimental values are presented in Figure 4 (dotted line). The agreement is, in general, remarkably good, considering that the prediction used a less number of experimental points in the regression. These results further recommend the predicting capabilities of Eqs. 2 and 7 for oils not considered in the data base. Again, the less-accurate results were obtained for Wells 7 and 8, where some experimental uncertainties may exist.

Figure 3a, shows data on bubble-point pressures of various Mexican live oils as a function of temperature. These data

Table 3. (a) Universal Slope and Composition-Dependent Correlation Parameters for Eqs. 2,7 (P^{upp}) and 8,9 (P^{bp}); (b) Illustration on the Change of Equation Parameters in (a) as a Result of Excluding the Data of Well 3

(a) Upper onset pressure equation coefficients		Bubble point pressure equation coefficients	
B^{upp} (MPa^{-1})	0,047408719	B^{bp} (K^{-1} MPa)	0,057778821
$f^{upp}_{H_2S}$ (K MPa^{-1})	−3,364315662	$f^{bp}_{H_2S}$ (K MPa^{-1})	−1,0265795
$f^{upp}_{N_2}$ (K MPa^{-1})	0,590476022	$f^{bp}_{N_2}$ (K MPa^{-})	−2,708388597
$f^{upp}_{CO_2}$ (K MPa^{-1})	−3,337934227	$f^{bp}{}_{CO_2}$ (K MPa^{-1})	8,593888235
$f^{upp}_{C_1-C4}$ (K MPa^{-1})	−1,125509198	f^{bp}_{sat} (K MPa^{-1})	0,308387207
f^{upp}_{sat} (K MPa^{-1})	1,325877421	f^{bp}_{arom} (Mpa^{-1})	−0,143981998
f^{upp}_{arom} (K MPa^{-1})	−0,515158363	f^{bp}_{res} (MPa^{-1})	−0,998941672
f^{upp}_{res} (K MPa^{-1})	0,576495619	f^{bp}_{asph} (MPa^{-1})	−2,98440823
f^{upp}_{asph} (K MPa^{-1})	2,118534736		
(b) Upper onset pressure equation coefficients for the prediction of well 3		Bubble point pressure equation coefficients for the prediction of well 3	
$f^{upp}_{H_2S}$ (K MPa^{-1})	−3,097711245	$f^{bp}_{H_2S}$ (K MPa^{-1})	−0,402390827
$f^{upp}_{N_2}$ (K MPa^{-1})	0,331878047	$f^{bp}_{N_2}$ (K MPa^{-1})	−1,293380632
$f^{upp}_{CO_2}$ (K MPa^{-1})	−3,513640644	$f^{bo}_{CO_2}$ (K MPa^{-1})	7,023442146
$f^{upp}_{C_1-C_4}$ (K MPa^{-1})	−1,082965758	f^{bp}_{sat} (K MPa^{-1})	0,252896906
f^{upp}_{sat} (K MPa^{-1})	1,266176029	f^{bp}_{arom} (MPa^{-1})	−0,166046852
f^{upp}_{arom} (K MPa^{-1})	−0,491411945	f^{bp}_{res} (MPa^{-1})	−0,850632386
f^{upp}_{res} (K MPa^{-1})	0,559401266	f^{bp}_{asph} (MPa^{-1})	−2,98440823
f^{upp}_{asph} (K MPa^{-1})	2,159488891		

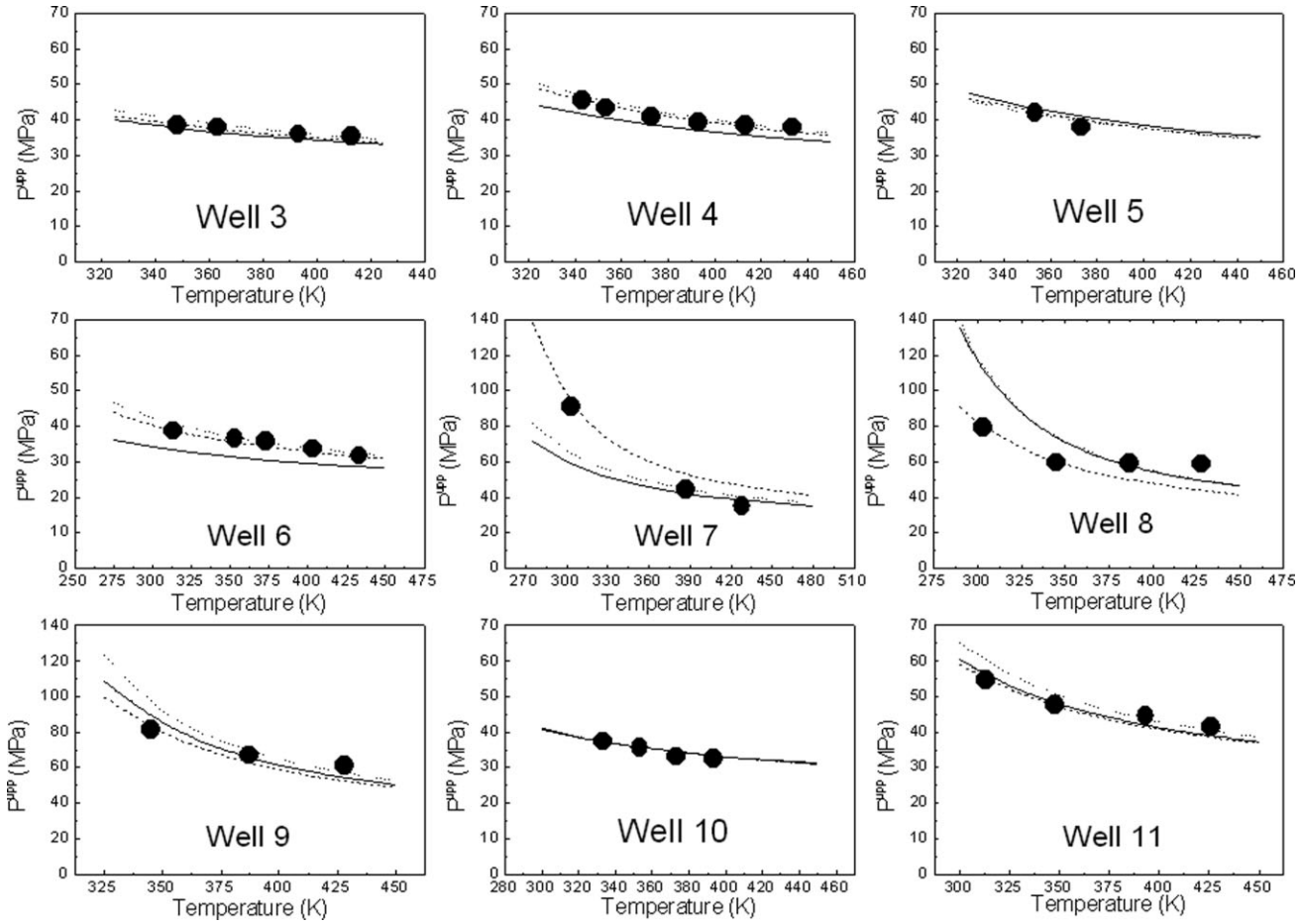

Figure 4. Calculated upper-onset of asphaltene precipitation pressures, P^{upp} for nine Mexican reservoir fluids.

Black circles are data shown in Table 1. The full-line represents calculations from Eqs. 2 and 7, including the data of the test Well (correlation); the dashed line are calculations from Eq. 11 (one-point approximation), and the dotted line are the calculated results from Eqs. 2 and 7, excluding the data of the test Well (predictive option).

were reduced using the modified least-squares procedure described in the Appendix. Table 3a shows the resulting values of the common slope, B^{bp} and correlation coefficients for the intercept, $f^{bp}(\boldsymbol{C}_{bp})$ for each crude (see Eq. 9). As Table 3b shows, these coefficients changed moderately when individual data sets were arbitrarily eliminated from the fits. Figure 5 shows values for P^{bp} from experimental data (dark circles); from Eqs. 8 and 9 by using the correlation coefficients shown in Table 3a (full line), and by excluding the experimental data of the oil of interest, as stated before (predictive manner, dotted line). The results of Figure 5 show that the agreement of Eqs. 8 and 9 is very good. The predicted results for Wells 4 were clearly less accurate. Table 4 shows the calculated AAD's for each oil. The average absolute deviation in predicted P^{bp} by Eqs. 8 and 9, is of 1.62 MPa.

Let us now examine an interesting property of Eq. 2. By assuming that a single experimental APE data point at P_o^{upp} and T_O is solely available from experiments, from Eq. 1, we have

$$f^{upp}(C_{\text{upp}}) = \frac{T_o}{P_o^{upp}} - B^{upp}T_o \tag{11}$$

Substituting Eq. 11 into Eq. 2 yields

$$P^{upp}(T) = \frac{T}{\frac{T_o}{P_o^{upp}} + B^{upp}[T - T_o]} \tag{12}$$

Table 4. Average Absolute Deviations, AAD's in Calculated Results of Figures 4 and 5

	Using composition-based correlations (i.e. Eqs. 2–7 and 8–9)		Using one-point expressions (i.e. Eqs. 11 and 13)	
	Onset point	Bubblepoint	Onset point	Bubblepoint
Well	AAD	AAD	AAD	AAD
1		0,74		0,62
2		2,27		0,19
3	0,47	3,44	0,65	0,78
4	0,74	0,29	0,78	0,99
5	1,09	0,58	1,00	0,58
6	0,69	2,08	0,85	0,34
7	11,08	1,30	6,65	0,29
8	13,05	0,59	6,15	0,23
9	5,75	2,00	4,43	0,31
10	0,57	2,94	0,57	0,20
11	2,24		1,66	

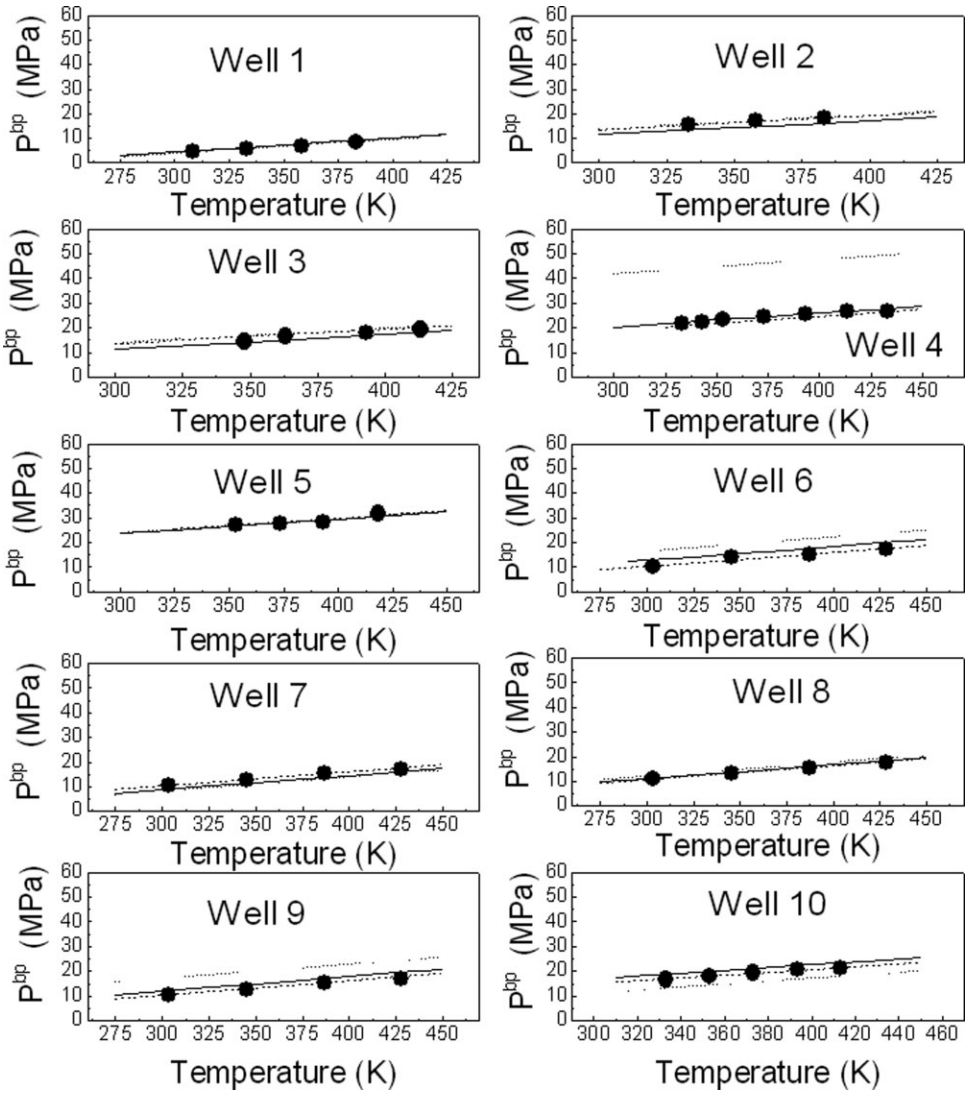

Figure 5. Predicted bubble-point pressures of 10 Mexican reservoir fluids as a function of temperature.

Black circles are data from Table 1. The dotted line are results from Eqs. 8–9, excluding the data of the test Well (predictive option); the full line are results of Eqs. 8–9, including the data of the test well (correlation), the dashed line are results from Eq. 13 (one-point approximation).

Equation 12 states that, from knowledge of a single experimental onset-pressure data pair P_o^{upp}, T_o one can predict the whole $P^{upp}(T)$ curve at any temperature T. Figure 4 also shows the results of the calculations using Eq. 11 (dashed lines), where the lower-temperature experimental value for $P^{upp}(T)$ was taken as P_o^{upp}, T_o. Results are also quite satisfactory, considering that only a single experimental data point is used to predict the entire phase boundary. AAD (see Table 4) from this expression is of 2.53 MPa. Similar to the case of P_o^{upp} in Eq. 12, if a single bubble-point pressure datum P_o^{bp}, at a given temperature T_o, is available from experimental information, one can use Eq. 8 to derive an equation to predict the whole bubble-point curve of a reservoir fluid as a function of temperature. The final expression is

$$P^{bp} = P_o^{bp} + B^{bp}[T - T_o] \tag{13}$$

Using Eq. 13, Table 4 shows that the calculated AAD are of 0.45 MPa. The results are graphically shown in Figure 5, where, in general, the results agree very well with the experimental information.

Table 5 shows the computed standard deviation of each parameter for the case of either Eqs. 2, 7 for P^{upp}, and Eqs. 8–9

Table 5. Calculated Parameter Standard Deviations

Upper onset pressure standard deviation in equation coefficients		Bubble point pressure standard deviation in equation coefficients	
B^{upp} (MPa^{-1})	0,016	B^{bp} (K^{-1} MPa)	0,0072
$f^{upp}_{H_2S}$ (K MPa^{-1})	0,13	$f^{bp}_{H_2S}$ (K MPa^{-1})	0,79
$f^{upp}_{N_2}$ (K MPa^{-1})	0,40	$f^{bp}_{N_2}$ (K MPa^{-1})	8,9
$f^{upp}_{CO_2}$ (K MPa^{-1})	0,11	$f^{bp}_{CO_2}$ (K MPa^{-1})	2,9
$f^{upp}_{C_1-C_4}$ (K MPa^{-1})	0,031	f^{bp}_{sat} (K MPa^{-1})	0,12
f^{upp}_{sat} (K MPa^{-1})	0,040	f^{bp}_{arom} (MPa^{-1})	0,12
f^{upp}_{arom} (K MPa^{-1})	0,018	f^{bp}_{res} (MPa^{-1})	0,30
f^{upp}_{res} (K MPa^{-1})	0,20	f^{bp}_{asph} (MPa^{-1})	1,4
f^{upp}_{asph} (K MPa^{-1})	0,064		

for P^{bp}. From this table, it can be seen that parameters $f_{N_2}^{upp}$, f_{res}^{upp}, have the less accuracy in upper onset pressure computations, while parameters $f_{N_2}^{bp}$, $f_{CO_2}^{bp}$ and $f_{H_2S}^{bp}$ have more influence on bubble pressure calculations by the proposed expressions. These results are based on statistical considerations.

Conclusions

Two algebraic equations to predict the onset and bubble-point pressures of asphaltene precipitation in reservoir fluids have been developed. The proposed equations are simple and have been derived from analysis of the onset/bubble-point pressure behavior of a number of live oils of different origin. With similar approximations, this method could be extended to predict the phase boundaries of other complex phase diagrams in crude oil (i.e., wax and hydrates). Depending of the amount of experimental data available for an oil, two working versions of the proposed equations are presented. Either in their shorter form (Eqs. 11 and 13 for P^{upp} and P^{bp}, respectively), or by means of a compositional correlation (Eqs. 2, 7 and 8, 9, respectively), the proposed expressions allow for a rapid, straightforward and accurate estimation of the onset/bubble-point pressures of asphaltenic live oils, as required in higher-level studies of flow assurance.

Complimentary Material Available

A Microsoft-Excel computer program to perform the calculations presented in this work is available from the authors upon request.

Acknowledgements

The authors thank the authorities of the Mexican Inst. of Petroleum in Mexico City, for permission to publish this work. Funding for this research from grant D.00403 is gratefully acknowledged.

Notation

B = correlation slopes
$\boldsymbol{C}$ = composition vector
T = temperature
P = pressure
x = mole fraction
t = weight fraction
W = number of subsets

Greek letters

$\chi^{2(K)}$ = χ^2 function of a straight line with index K in Eq. A2 (Appendix)

Subscripts

upp = upper
sat = saturates
$arom$ = aromatics
res = resins
$asph$ = asphaltenes
bp = bubble point
To = reference temperature
Po = reference pressure
N,n = number of data

Superscripts

upp = upper
bp = bubble point

Functions

f = function of composition

Literature Cited

1. Leontaritis KJ. The asphaltene and wax deposition envelopes. *Fuel Sci Tech Int*. 2006;14:13–39.
2. Lira-Galeana C, Hammami A. *Wax Precipitation from Petroleum Fluids. A Review*. In: *Asphaltenes and Asphalts II*. Yen TF, Chilingarian G, eds. *(Chapter 21)*. The Netherlands: Elsevier Science Publisher; 2000.
3. Shields D. *Offshore*. 2000;60(9):84–86.
4. Fahim MA. Empirical equations for estimating ade of crude oils. *Petrol Sci Technol*. 2007;25:949–965.
5. Fahim MA. Prediction of asphaltene precipitation from empirical models. *Petrol Sci Technol*. 2007;25:1605–1612.
6. Fahim MA, Andersen SI. Tuning EOS using molecular thermodynamics construct asphaltene deposition envelope (ADE), paper 93517 presented at the 14th Middle East Oil and Gas Show and Conference of the Society of Petroleum Engineers; March 12–15, 2005; Bahrain International Exhibition Centre, Bahrain, SA.
7. Aquino-Olivos MA, Buenrostro-Gonzalez E, Andersen SI, Lira-Galeana C. Investigations of inhibition of asphaltene precipitation at high pressure using bottomhole Samples. *Energy Fuels*.15;1:236.
8. Aquino-Olivos MA, Lira-galeana C, Andersen SI. Comparisons between asphaltenes from the dead and live-oil samples of the same crude oils. *Pet Sci Technol*. 2003;21(5&6):1017.
9. Buenrostro-Gonzalez E, Lira-Galeana C, Gil-Villegas A, Wu J. Asphaltene precipitation in crude oils: theory and experiments. *AIChE J*. 2004;50:2552–2570.
10. Hammami A, Phelps H, Little TM. Asphaltene precipitation from live oils: an experimental investigation of the onset conditions and reversibility. *Energy Fuels*. 2000;14:14.
11. Ramirez-Jaramillo E, Manero O, Lira-Galeana C. Modeling asphaltene deposition in production pipelines. *Energy Fuels*. 2006;20(3):1184.
12. Islas-Flores C, Buenrostro-Gonzalez E, Lira-Galeana C. Comparisons between open column chromatography and hplc-sara fractionantions in petroleum. *Energy Fuels*. 2005:19(5):2001.

Appendix

A modified version of the least-squares regression

Let us have a set of data points (see Figure A1) of a number of W subsets. If N_k is the number of data points of the k-th subset, each subset has a number of data pairs of the type $(x_i^{(k)}, y_i^{(k)})$, $i = 1,\ldots,N_k$. We will fit such data set to a set of parallel straight lines of the form

$$y^{(k)} = Bx + f^{(k)} \tag{A1}$$

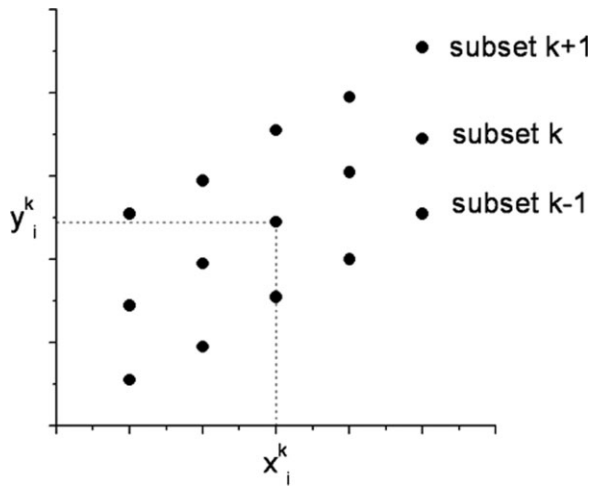

Figure A1. Data sets and subsets.

where $k = 1,\ldots W$. In Eq. A1, B is the common slope of the parallel straight lines, while $f^{(k)}$ will vary depending on the subset under consideration. For the k-th subset, we can define $\chi^{2(k)}$ by

$$\chi^{2(k)} = \sum_{i=1}^{N_k} \left(y_i^{(k)} - B x_i^{(k)} - f^{(k)} \right)^2 \tag{A2}$$

One should consider that

$$\chi^{2(k)} = \chi^{2(k)}(B, f^{(k)}) \tag{A3}$$

In this way, we can define χ^2 for the whole set by

$$\chi^2 = \chi^2\left(\mathrm{B}, f^{(1)}, f^{(1)}, \ldots, f^{(k)}\right) = \sum_{k=1}^{W} \chi^{2(k)}\left(\mathrm{B}, f^{(k)}\right) \tag{A4}$$

Since a set of straight lines of the form given by Eq. A1 that provides the best fit to the data set of Figure 6 is sought, we will get the set of parameters B, $f^{(1)},\ldots f^{(k)}$ such that the value of χ^2 is minimized. That is, we will look for the set of parameters that solve the following system of equations

$$\begin{aligned} \left(\frac{\partial \chi^2}{\partial \mathrm{B}}\right) &= \sum_{k=1}^{W} \left(\frac{\partial \chi^{2(k)}}{\partial \mathrm{B}}\right) = 0 \\ \left(\frac{\partial \chi^2}{\partial f^{(k)}}\right) &= \left(\frac{\partial \chi^{2(k)}}{\partial \mathrm{f}^{(k)}}\right) = 0 \end{aligned} \tag{A5}$$

where $k = 1,\ldots,W$. Substituting Eq. A2 in A5, and by considering that

$$\begin{aligned} \left\langle x_i^{(k)} y_i^{(k)} \right\rangle &= \frac{1}{N_k} \sum_{i=1}^{N_k} x_i^{(k)} y_i^{(k)} \\ \left\langle y_i^{(k)} \right\rangle &= \frac{1}{N_k} \sum_{i=1}^{N_k} y_i^{(k)} \\ \left\langle x_i^{(k)} \right\rangle &= \frac{1}{N_k} \sum_{i=1}^{N_k} x_i^{(k)} \\ \left\langle (x_i^{(k)})^2 \right\rangle &= \frac{1}{N_k} \sum_{i=1}^{N_k} (x_i^{(k)})^2 \end{aligned} \tag{A6}$$

we have

$$\sum_{k=1}^{W} N_k \left\langle x_i^{(k)} y_i^{(k)} \right\rangle = \mathrm{B} \sum_{k=1}^{W} N_k \left\langle (x_i^{(k)})^2 \right\rangle + \sum_{k=1}^{W} N_k f^{(k)} \left\langle x_i^{(k)} \right\rangle \tag{A7}$$

$$\left\langle y_i^{(k)} \right\rangle = \mathrm{B} \left\langle x_i^{(k)} \right\rangle + f^{(k)} \tag{A8}$$

Substituting A8 into A7, we have

$$\mathrm{B} = \frac{\sum_{k=1}^{W} N_k \left[\left\langle x_i^{(k)} y_i^{(k)} \right\rangle - \left\langle x_i^{(k)} \right\rangle \left\langle y_i^{(k)} \right\rangle \right]}{\sum_{k=1}^{W} N_k \mathrm{var}(x_i^{(k)})} \tag{A9}$$

where

$$\mathrm{var}(x_i^{(k)}) = \left\langle (x_i^{(k)})^2 \right\rangle - \left\langle x_i^{(k)} \right\rangle^2 \tag{A10}$$

If the k-th subset is fitted in an independent manner to a straight line using the least-squares method, the resulting value of the slope is

$$\mathrm{b}^{(k)} = \frac{\left\langle x_i^{(k)} y_i^{(k)} \right\rangle - \left\langle x_i^{(k)} \right\rangle \left\langle y_i^{(k)} \right\rangle}{\mathrm{var}(x_i^{(k)})} \tag{A11}$$

From Eq. A11 and substituting in Eq. A9

$$\mathrm{B} = \frac{\sum_{k=1}^{W} N_k \mathrm{var}(x_i^{(k)}) \mathrm{b}^k}{\sum_{k=1}^{W} N_k \mathrm{var}(x_i^{(k)})} \tag{A12}$$

For the sake of easier programming, we may make two assumptions. The first assumption states that all subsets have a similar number of points. That is

$$N_1 \approx N_2 \approx .... \approx N_W \approx N \tag{A13}$$

The second assumption states that all k-th subsets have been considered on similar space intervals on the X-axe. In that way

$$\begin{aligned} \mathrm{var}(x_i^{(1)}) \approx \mathrm{var}(x_i^{(2)}) \approx \mathrm{var}(x_i^{(3)}) \approx ..... \approx \mathrm{var}(x_i^{(k)}) \\ \approx ..... \approx \mathrm{var}(x_i^{(W)}) \approx \mathrm{var}(x_i) \end{aligned} \tag{A14}$$

By substituting Eqs. A13 and A14 in Eq. A12

$$\mathrm{B} = \frac{\sum_{k=1}^{W} \mathrm{b}^k}{W} \tag{A15}$$

That is, the common slope for the set is the average slope that would result from performing individual fits to each subset. From Eq. A8

$$f^{(k)} = \left\langle y_i^{(k)} \right\rangle - \mathrm{B} \left\langle x_i^{(k)} \right\rangle \tag{A16}$$

This equation allows us to compute the value of $f^{(k)}$ for each subset from knowledge of the value of B.

Manuscript received Sept. 9, 2008, and revision received Feb. 4, 2009.